# Ferromagnetism in the vicinity of Lifshitz topological transitions

P. S. Grigoryev,[1,*] M. M. Glazov,[2,1] A. V. Kavokin,[3,4,1] and A. A. Varlamov[3]
[1]*Spin Optics Laboratory, St. Petersburg State University, Ulyanovskaya 1, 198504 St. Petersburg, Russia*
[2]*Ioffe Institute, 26 Polytechnicheskaya Street, 194021 St. Petersburg, Russia*
[3]*CNR-SPIN, Tor Vergata, Viale del Politecnico 1, I-00133 Rome, Italy*
[4]*School of Physics and Astronomy, University of Southampton, Southampton SO17 1BJ, United Kingdom*
(Received 16 June 2017; revised manuscript received 7 September 2017; published 9 November 2017)

We show that the critical temperature of the ferromagnetic phase transition in a quasi-two-dimensional hole gas confined in a diluted magnetic semiconductor quantum well strongly depends on the hole chemical potential and hole density. Significant variations of the Curie temperature occur close to the Lifshitz topological transition points, where the hole Fermi surface acquires additional components of topological connectivity due to the filling of excited size-quantization subbands. The model calculations demonstrate that the Curie temperature can be doubled by a weak variation of the gate voltage for a CdMnTe/CdMgTe quantum-well-based device.

DOI: 10.1103/PhysRevB.96.205415

## I. INTRODUCTION

Quantum wells (QWs) based on diluted magnetic semiconductors (DMS) have been attracting attention for several decades due to their unusual magneto-optical properties [1–3]. One of the most interesting observed effects that is potentially promising for applications in semiconductor spintronics is carrier-induced ferromagnetism [4,5]. Magnetic ordering of the spins of magnetic ions may occur due to their exchange interaction with spins of delocalized carriers, typically holes. In particular, the doping of III-V semiconductors by $Mn^{2+}$ ions results in formation of acceptor states [6], or even impurity bands in the case of heavy doping [7–10]. The holes coming from these acceptors help in achieving ferromagnetic ordering at elevated temperatures [11].

Ferromagnetic ordering of spins of magnetic ions at relatively low concentrations (several percent) can be described in terms of the Ruderman-Kittel-Kasuya-Yosida (RKKY) mechanism. The record Curie temperature achieved due to this mechanism in III-V semiconductors doped with Mn reaches hundreds of Kelvin [11,12] for the best quality samples. The most optimistic theoretical estimates predict ferromagnetism in GaMnAs at moderate Mn concentrations even at room temperature [11]. Yet, it turns out that a significant amount of holes are compensated due to the interstitial Mn incorporation [13] that reduces the ferromagnetic transition temperature.

In contrast to III-V semiconductors, in II-VI semiconductors Mn ions do not form acceptor states. Therefore they weakly affect the band structure of the host semiconductor. This is why, when describing the coupling of magnetic ion spins with carriers in II-VI semiconductors, one can rely on a symmetry-based band description. This allows for a straightforward description of the electronic properties of diluted magnetic QWs.

The correlation between the RKKY interaction strength and the carrier density of states in bulk crystals is well known [14,15]. It was confirmed theoretically for carriers with a parabolic dispersion in systems of arbitrary dimension [16,17]. Studies of DMS structures also revealed this correlation both experimentally [4,18] and theoretically [19,20]. It was also shown that the Curie temperature is proportional to RKKY interaction strength, and consequently to the density of states. The electronic density of states can be efficiently controlled by an external bias in quantum confined semiconductor structures [21]. This paves way to an efficient control of the Curie temperature with an external electric field in specially designed diluted magnetic quantum structures. We note that the variation of the Curie temperature with the external bias has been also demonstrated in bulk systems [22]. Here we argue that a similar effect, but of a much larger magnitude, may be realized in diluted magnetic quantum wells, where the Fermi level approaches the electronic topological transition point.

In particular, we show that the critical conditions for the ferromagnetic phase transition in the studied system become extremely sensitive to the chemical potential of the hole gas in the vicinity of topological transition points in the valence band. This opens the way for efficient control of the Curie temperature in such structures by an external bias. Switching on and off the ferromagnetism may be achieved by a weak variation of voltage applied to a properly designed diluted magnetic QW. This property, based on the fundamental physics of Lifshitz topological transitions, may open the way to realization of a new class of spintronic devices.

It is well known that once the electronic chemical potential crosses the bottom of one of the size-quantization subbands in a quantum well, the Fermi surface acquires a new component of topological connectivity. This transition is a particular case of the Lifshitz topological transition [23]. It was recently demonstrated that such transformations are accompanied by spikes in the entropy per particle as well as by spikes in the temperature derivative of the chemical potential of the electron or hole gas [24]. Below we show that the magnetic susceptibility of the system experiences similar spikes in the vicinity of the Lifshitz transition points. This leads to a very strong variation of the Curie temperature with a weak variation of the chemical potential of the hole gas that may be achieved by the application of an external bias.

## II. MODEL

Let us consider a CdMnTe/CdMgTe QW, embedded in a gated structure schematically shown in Fig. 1. The gate voltage

*f.grigoriev@spbu.ru

 

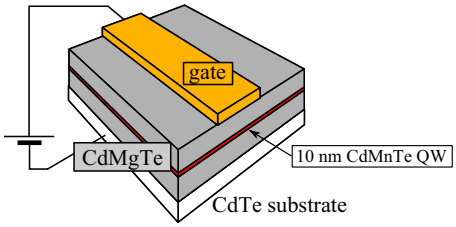


FIG. 1. The considered model structure contains a single CdMnTe QW sandwiched between CdMgTe barriers. The gate voltage applied to the structure controls the concentration of holes in the QW.

$U_g$ applied to the structure controls the density of the two-dimensional hole gas (2DHG) confined in the QW, $n_h$. Within a linear approximation, $n_h = CU_g/|e|$, where $e$ is the electron charge and $C$ is the structure capacitance. In what follows, for simplicity we assume that the capacitance $C$ is independent of the gate voltage and it is governed by the geometry of the structure rather than by the density of states [25,26].

A ferromagnetic ordering of the Mn ions' magnetic momenta is possible due to the RKKY interaction between the ion spins mediated by the 2DHG [1–5]. Due to the exchange interaction between the hole and Mn spins, the fluctuations of the latter give rise to hole spin polarization which, in turn, provides positive feedback to the Mn spin system. Quantitatively, in bulk semiconductors the exchange interaction of $d$ electrons of Mn ions with the hole spin is described by the effective Hamiltonian [2,3,27]

$$\mathcal{H}_{\rm exch} = -\sum_i J_{pd}\delta(\boldsymbol{r}-\boldsymbol{R}_i)(\boldsymbol{J}\cdot\boldsymbol{I}_i), \tag{1}$$

where $J_{pd}$ is a constant, $\boldsymbol{J}$ are the matrices of the hole angular momentum 3/2, $\boldsymbol{I}_i$ are the Mn spin operators described by the spin-5/2 matrices, and the summation is carried out over all Mn ions enumerated by the subscript $i$. In Eq. (1), $\boldsymbol{r}$ and $\boldsymbol{R}_i$ are the position vectors of the hole and $i$th Mn, respectively. In a QW structure, Eq. (1) should be averaged over appropriate size quantization states. Hereafter we consider only heavy- and light-hole states and disregard the spin-orbit split-off branch due to significant energy separation between the $\Gamma_8$ and $\Gamma_7$ valence bands [28]. We assume that the system shown in Fig. 1 contains a symmetric QW grown along the $z \parallel [001]$ axis. Diagonalizing the Hamiltonian (1), we obtain a series of the heavy- and light-hole subbands, $hh\nu$ and $lh\nu$, respectively, with $\nu = 1,2,\ldots$, with corresponding envelope functions $\varphi_{hh\nu}(z)$, $\varphi_{lh\nu}(z)$. The exchange interaction of the heavy and light holes with magnetic ions is described by

$$\mathcal{H}_{\rm hh} = -\sum_i J_{hh\nu,i}(s_{hh,z}I_{i,z})\delta(\boldsymbol{\rho}-\boldsymbol{\varrho}_i), \tag{2a}$$

$$\mathcal{H}_{\rm lh} = -\sum_i J_{lh\nu,i}[s_{lh,z}I_{i,z} + 2(s_{lh,x}I_{i,x} + s_{lh,y}I_{i,y})] \times \delta(\boldsymbol{\rho}-\boldsymbol{\varrho}_i). \tag{2b}$$

Here $J_{hh\nu,i} = 3J_{pd}|\varphi_{hh\nu}(z_i)|^2$, $J_{lh\nu,i} = J_{pd}|\varphi_{lh\nu}(z_i)|^2$, $\boldsymbol{\rho}$ and $\boldsymbol{\varrho}_i$ are the in-plane position vectors of the hole and $i$th Mn ion, $s_{hh,z}$ is the $z$ component of the heavy-hole pseudospin ($s_{hh,z} = \pm 1/2$ for $J_z = \pm 3/2$), and $s_{lh}$ is the light-hole pseudospin. Note that in QW structures the exchange interaction is anisotropic both for the heavy and light holes. A particularly strong anisotropy is found for the heavy holes, where the interaction described by Eq. (2a) acquires the Ising form.

In order to illustrate the appearance of the magnetic phase transition and estimate the Curie temperature $T_c$ in the Mn spin system we use the mean field approach. We take into account only interaction between $z$-spin components of Mn ions and holes, and represent the thermodynamic potential in the form

$$\Phi = \frac{I_z^2}{2\chi^{(\rm Mn)}} + \frac{s_{hh,z}^2}{2\chi^{(hh)}} + \frac{s_{lh,z}^2}{2\chi^{(lh)}} - I_z(J_{hh}s_{hh,z} + J_{lh}s_{lh,z}) + \mu_B B_z(g_{\rm Mn}I_z + g_{hh}s_{hh,z} + g_{lh}s_{lh,z}), \tag{3}$$

where $g_{\rm Mn}$, $g_{hh}$, and $g_{lh}$ are the Mn and hole $g$ factors, respectively; $\mu_B$ is the Bohr magneton; $B_z$ is the $z$ component of the external magnetic field; $I_z$, $s_{hh,z}$, and $s_{lh,z}$ are the spin densities of Mn, heavy, and light holes; and $J_{hh}$ and $J_{lh}$ are the averaged exchange interaction constants for the corresponding hole states [29]. Here $\chi^{(\rm Mn)}$ is the noninteracting susceptibility of Mn ions,

$$\chi^{(\rm Mn)} = \frac{I(I+1)n_{\rm Mn}}{3k_BT}, \tag{4}$$

with $I = 5/2$ being the Mn spin and $n_{\rm Mn}$ the density of Mn ions on the sample, and $\chi^{(hh)}$ and $\chi^{(lh)}$ are the static susceptibilities of the heavy and light holes. Note that the susceptibilities defined here provide the link between the spin density and the field-induced level splitting, e.g., $I_z = -\chi^{(\rm Mn)}g_{\rm Mn}\mu_B B_z$.

In Eq. (3) we take into account only contributions linear and quadratic in $I_z$, $s_{hh,z}$, and $s_{lh,z}$, neglecting the magnetization and magnetic field effect on the susceptibilities. This is valid as long as the exchange energy is small compared to the hole size-quantization and kinetic energies, while the exchange energy can become comparable with the temperature. Estimations show that this condition is also fulfilled in the system under consideration.

Minimizing $\Phi$ with respect to $I_z$, $s_{hh,z}$, and $s_{lh,z}$ allows us to obtain the effective susceptibility of the Mn spin system as

$$\tilde{\chi}^{(\rm Mn)} = \frac{\chi^{(\rm Mn)}}{1-\left(J_{hh}^2\chi^{(hh)} + J_{lh}^2\chi^{(lh)}\right)\chi^{(\rm Mn)}}. \tag{5}$$

Since, in accordance to the fluctuation-dissipation theorem, the spin susceptibility is proportional to the spin-spin correlation function [30], $\tilde{\chi}^{(\rm Mn)} = \mathcal{S}\langle I_z^2\rangle/k_BT$, where $\mathcal{S}$ is the normalization area, the divergence of the susceptibility corresponds to the phase transition point. It follows from Eqs. (4) and (5) that the divergence occurs where the denominator vanishes, which yields the self-consistent equation for the Curie temperature [2–4],

$$T_c = \frac{I(I+1)n_{\rm Mn}}{3k_B}\left(J_{hh}^2\chi^{(hh)} + J_{lh}^2\chi^{(lh)}\right). \tag{6}$$

The expression (6) is valid provided that $k_BT_c \ll \mu$, where $\mu$ is the hole chemical potential, otherwise the ground state of the hole gas is strongly modified by the exchange interaction with magnetic ions. Calculations show that this condition is indeed fulfilled for the studied structure.

We follow the standard approach [30] to analyze the applicability of the mean-field treatment. We consider a

fluctuation of the thermodynamic potential given by

$$\delta\Phi = g\left(\frac{\partial s_z}{\partial \boldsymbol{r}}\right)^2 + \frac{bI_z^4}{2\chi^{(\mathrm{Mn})}}, \tag{7}$$

where $g$ and $b$ are constants. The parameter $b$ can be found from the development of the Brillouin function in a series and retaining the cubic terms: $b = (I^2 + I + 1/2)/[10I(I+1)n_{\mathrm{Mn}}^2]$. For long wavelength fluctuations with wave vector $\boldsymbol{q}$, the effective Mn susceptibility reads [cf. Eq. (5)]

$$\tilde{\chi}_{\boldsymbol{q}}^{(\mathrm{Mn})} \approx \frac{\chi^{(\mathrm{Mn})}}{1 + (ql_s)^2 - T_c/T}. \tag{8}$$

Here $l_s = \sqrt{g\chi^{(h)}}$. This approximate equality holds for $T - T_c \ll T_c$ and $ql_s \ll 1$. Equation (8) allows one to obtain the correlation radius of fluctuations (above $T_c$) in the standard form

$$r_c = \frac{l_s}{\sqrt{1 - T_c/T}}. \tag{9}$$

Note that the applicability of the mean field approximation is restricted by the requirement of the relative weakness of the spin density fluctuations. Namely, the mean square fluctuation of $I_z$ per unit square, $\delta I_z^2 \sim k_B T_c \tilde{\chi}^{(\mathrm{Mn})}/r_c^2$, must be small with respect to the average value of the spin density square $I_z^2$. The latter is obtained in the mean field approximation, i.e., by means of minimization of the functional $\Phi + \delta\Phi$ [see Eqs. (3) and (7)] omitting the fourth-order term: $I_z^2 = (T_c - T)/(2bT_c)$. This analysis brings us to the conclusion that the mean field approximation is valid in the temperature range given by

$$\mathrm{Gi} \ll \frac{|T - T_c|}{T_c} \ll 1, \tag{10}$$

where the quantity $\mathrm{Gi} = (n_{\mathrm{Mn}} l_s^2)^{-1}$ plays the role of the Ginzburg-Levanyuk number [30] in the two-dimensional case under consideration. One can see that the inequality (10) is fulfilled in diluted magnetic CdTe-based QWs. Indeed, the parameter $l_s$ for free holes at low temperatures can be estimated as $l_s \sim k_F^{-1}$, where $k_F$ is the hole wave vector. Hence, the condition $\mathrm{Gi} \ll 1$ means that the density of holes is low in comparison to the density of Mn ions, which is always the case. For example, in our case minimal 1% Mn concentration corresponds to $\approx 10^{14}$ cm$^{-2}$, and hole concentration usually does not exceed $10^{13}$ cm$^{-2}$.

For a noninteracting hole gas, the susceptibility can be written as [30]

$$\chi^{(h)} = -\frac{1}{4\mathcal{S}}\frac{\partial^2\Omega^{(j)}}{\partial\mu^2} = \frac{1}{4}\frac{\partial n_j}{\partial\mu}. \tag{11}$$

where $\Omega^{(j)} \equiv \Omega^{(j)}(\mu)$ is the (grand) thermodynamical potential, $\mu$ is the chemical potential, and $n_j$ is the density of the corresponding hole states, $j = hh$ or $lh$. The latter can be conveniently expressed in terms of the density of the hole states, $g_h(E)$, as

$$n_h = \int_0^\infty \frac{g_h(E)dE}{\exp\left(\frac{E-\mu}{k_BT}\right) + 1}, \tag{12}$$

where the energy is reckoned from the $hh1$ subband size quantization energy. In what follows, Eqs. (11) and (12) are used to numerically calculate the susceptibilities of the hole gas as functions of temperature and the hole density and to solve Eq. (6) in order to find the Curie temperature $T_c$ as a function of the hole density or gate voltage.

Before presenting the numerical results, let us focus on the simplified analytical model, which takes into account only one type of holes but provides a clear physical picture of the effect of topological Lifshitz transitions on the hole spin susceptibility and the ferromagnetic order of Mn spins. Let us represent the density of heavy-hole states as $g(E) = (m^*/\pi\hbar^2)\sum_\nu \Theta(E - E_{hh\nu})$, where $m^*$ is the heavy-hole effective mass, $E_{hh\nu}$ are the energies of the size-quantized subbands, and $\Theta(E)$ is the Heaviside step function [24,25]. Furthermore, let us assume that relevant temperatures are low enough so that the thermal broadening in Eq. (12) can be disregarded and the heavy-hole susceptibility can be recast in the form

$$\chi^{(hh)} = \frac{g(\mu)}{4} = \frac{m^*}{4\pi\hbar^2}\sum_\nu \Theta(\mu - E_{hh\nu}). \tag{13}$$

It follows from Eq. (6) that the Curie temperature $T_c \propto J_{hh}^2 n_{\mathrm{Mn}} \chi^{(hh)}(\mu)$ as a function of the hole chemical potential $\mu$ demonstrates a steplike increase as soon as $\mu$ touches the next heavy-hole subband. This is because the hole Fermi surface acquires a new component of topological connectivity, giving rise to the Lifshitz phase transition. It is accompanied by the steplike increase of the density of states since with further increase of the chemical potential more subbands start to get filled [23]. Hence, the Curie temperature increases by a certain value at the point of the Lifshitz transition. These results are corroborated by the numerical analysis below. We note, however, that Eq. (13) cannot be used in the narrow vicinity of the topological transition point where $|\mu - E_{hh\nu}| \lesssim k_BT$. The kinks in the $T_c(\mu)$ dependence predicted by Eqs. (6) and (13) are smoothed out, as shown below, due to the thermal broadening of the electron distribution function.

## III. RESULTS AND DISCUSSION

Figure 2 shows the results of numerical calculations for a 10-nm thick CdMnTe/CdMgTe QW. In order to find the energy dispersion of the heavy and light holes ($hh\nu$ and $lh\nu$ subbands, respectively) and the corresponding effective exchange interaction constants $J_{hh\nu}$ and $J_{lh\nu}$, we have numerically diagonalized the Luttinger Hamiltonian in a way similar to that in [31,32]. We made use of the fact that, at zero in-plane hole wave vector $\boldsymbol{k}_\parallel$, the states with $|J_z| = 3/2$ (heavy holes) and $|J_z| = 1/2$ (light holes) are decoupled. Hence, we first found the heavy- and light-hole functions $\varphi_{hh\nu}(z)$ and $\varphi_{lh\nu}(z)$ at $\boldsymbol{k}_\parallel = 0$. Second, we represented the hole wave functions at $\boldsymbol{k}_\parallel \neq 0$ as linear combinations of $\varphi_{hh\nu}(z)$ and $\varphi_{lh\nu}(z)$, and diagonalized the obtained matrix Hamiltonian. The calculated densities of states and energy dispersions for the hole subbands are shown in Fig. 2, panels (a) and (b) respectively.

In the studied range of energies, the heavy- and light-hole states are substantially mixed due to the off-diagonal elements of the Luttinger Hamiltonian. This results in the energy nonparabolicity and anticrossing behavior of the dispersion curves presented in Fig. 2(b). To illustrate the mixing in more detail we present in Fig. 2(a) the partial contributions of the heavy and light holes to the total density of states, calculated

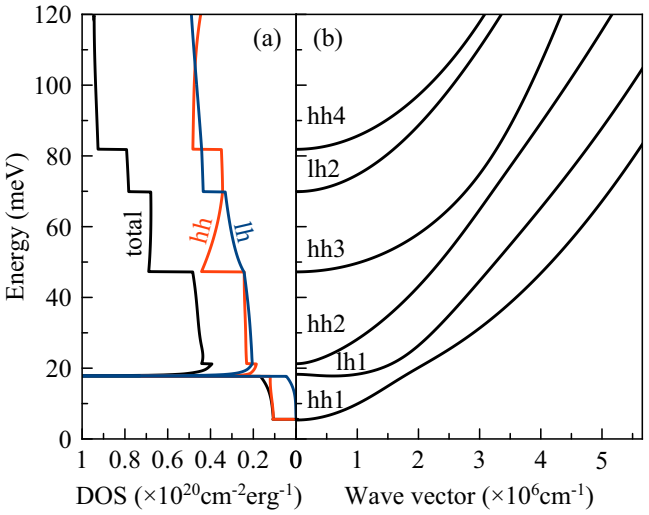


FIG. 2. (a) Densities of hole states in a 10-nm CdMnTe/CdMgTe QW (black) and the partial contributions of the heavy- (red) and light-hole (blue) states to the density of states. (b) Subbands of size quantization in a 10-nm CdMnTe/CdMgTe QW. In the calculation we used five basic functions for heavy and light holes and a spherical approximation for the Luttinger Hamiltonian with the parameters $\gamma_1 = 5.7$, $\gamma_2 = \gamma_3 = 1.7$ [28] and a barrier height of 120 meV.

as

$$g_{hh(lh)}(E) = \frac{1}{4\pi}\sum_{\nu}\frac{dk_\parallel^2}{dE}\mathcal{C}^{(\nu)}_{hh(lh)}(k_\parallel), \tag{14}$$

where the summation is carried out over all dispersion branches at a given energy, $\mathcal{C}^{(\nu)}_{hh(lh)}(k_\parallel)$ is the fraction of the corresponding heavy ($hh$) or light ($lh$) hole state in the subband state $\nu$, and $\mathcal{C}^{(\nu)}_{hh}(k_\parallel) + \mathcal{C}^{(\nu)}_{lh}(k_\parallel) = 1$. Note that in the spherical approximation employed here the dispersion is isotropic in the QW plane.

The results of this calculation, presented in Fig. 2(a), show the steplike behavior of the density of states. Moreover, the total density of states as well as the partial contributions of the heavy and light holes demonstrate sharp peaks followed by shallow minima in the vicinity of the onset of the first and second excited subbands; see $lh1$ and $hh2$ subbands in Fig. 2(b) and the density of states in the vicinity of ≈20 meV hole energy in panel (a). This result is a hallmark of heavy-light hole mixing, which is a specific feature of the II-VI and III-V semiconductors. For the parameters of the studied structure, the ground light-hole subband and the excited heavy-hole subband are close in energy and are strongly mixed via the off-diagonal $\propto -ik_\parallel\partial/\partial z$ terms of the Luttinger Hamiltonian. This mixing can be described within the two-subband approximation, where the effective $2\times 2$ Hamiltonian describing the $hh2$-$lh1$ doublet has the form

$$\mathcal{H}_{lh}(\boldsymbol{k}) = \begin{pmatrix} E_{hh2} + \frac{\hbar^2k^2}{2m_{hh}} & \hbar vk \\ \hbar vk & E_{lh1} + \frac{\hbar^2k^2}{2m_{lh1}} \end{pmatrix}. \tag{15}$$

Here $\boldsymbol{k}$ is the hole wave vector in the QW plane, $E_{hh2}$, $E_{lh1}$ are the energies of size quantization of holes calculated at $\boldsymbol{k} = 0$, $v$ is the parameter describing the hole mixing, $m_{hh} \propto (\gamma_1 + \gamma_2)^{-1}$ and $m_{lh} \propto (\gamma_1 - \gamma_2)^{-1}$ are the heavy- and light-hole in-plane effective masses calculated neglecting the heavy-light hole mixing, and $v \propto \gamma_2\langle hh2|k_z|lh1\rangle$. The Hamiltonian (15) provides a small-$\boldsymbol{k}$ approximation to the $4\times 4$ Luttinger Hamiltonian. The Hamiltonian (15) can be easily diagonalized with the energies

$$E_\pm = \frac{E_{hh2} + E_{lh1} + \hbar^2k^2/2\mu}{2} \pm \sqrt{\left(\frac{E_{hh2} - E_{lh1} + \hbar^2k^2/2M}{2}\right)^2 + \hbar^2v^2k^2}. \tag{16}$$

Here $1/\mu = 1/m_{hh} + 1/m_{lh}$, $1/M = 1/m_{hh} - 1/m_{lh}$. The dispersion $E_-(k)$ of the low-energy branch is, in general, a nonmonotonic function of the wavevector and has, in agreement with Fig. 2(b), minima at $|\boldsymbol{k}| = k_0$. In the vicinity of the minima it can be approximated as $E_{lh1} \approx \hbar^2E_m + (k - k_0)^2/2m^*$, where $E_m$ is the bottom of the first excited subband and $k_0$ is the wave vector corresponding to the subband bottom. As a result, the extremum loop is formed as seen in Fig. 3, where in panels (a), (b), and (c) the cuts of energy dispersion surfaces at different energies are presented. The density of states has a one-dimensional-like singularity $\propto 1/\sqrt{E - E_m}$, in agreement with the numerical calculation. Note that the singularly can be strongly enhanced by the interface-induced heavy-light hole mixing resulting from the chemical bond anisotropy in cubic crystalline lattices [33]. At somewhat higher energies an effective gap is formed between the first and second excited subbands, which results in a minimum of the density of states.

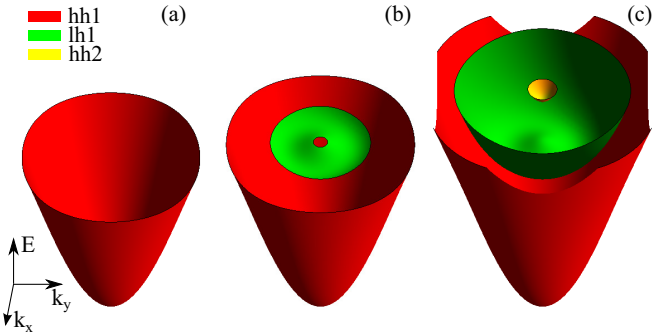


FIG. 3. The schematic illustration of the hole dispersion surfaces cut by the Fermi energy in the cases of the Fermi energy lying below the second hole subband bottom (a), below the third hole subband bottom (b), and above the third hole subband bottom (c).

Let us now discuss the Curie temperature dependence on the hole density or gate voltage in the QW structure, presented in Fig. 4. In the calculation we took the following values of the exchange interaction constants in Eq. (5): $J_{hh} = 3J_{lh} = 3J_{p-d}$, with $J_{p-d} = 59$ meV nm$^3$ being the $p$-$d$ exchange integral in the CdTe semiconductor [1–3]. In order to relate the gate voltage $V_g$ and the hole density $n$, we used the plane capacitor relation $n = CV_g/e$, where $e > 0$ is elementary charge and the capacitance $C = 20$ nF/cm$^2$ ($C/e = 1.25\times 10^{11}$ cm$^{-2}$/V). The chosen capacitance is close to the real observable value in CdTe solar cells [34].

Figure 4 shows that each Lifshitz transition in the system is accompanied by a steplike increase in the Curie temperature.

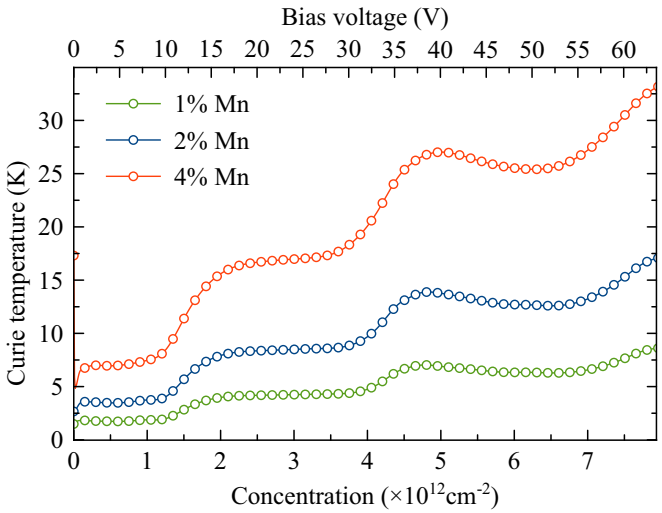


FIG. 4. Dependence of the Curie temperature on the bias voltage and the hole concentration for three values of the Mn concentration in the QW; $J_{hh} = 3J_{lh} = 3 \times 59$ meV nm$^3$, device capacitance $C = 20$ nF/cm$^2$.

In particular, the Curie temperature doubles with the bias voltage, changing between 10 and 15 V. As expected, the Curie temperature increases as the Mn content in the QW increases [35], which makes steps in the dependence of $T_c$ on the gate voltage or hole density more pronounced. Due to the thermal spread of the hole Fermi-Dirac distribution functions, the steps in the $T_c$ dependence seen in Fig. 2(a) are smooth. For the parameters used in the calculation, the square-root singularity in the density of states in the vicinity of the first and second excited subbands is not reproduced in the $T_c$ dependence on the hole density. The numerical analysis shows that the heavy-light hole mixing should be unrealistically high to obtain a pronounced nonmonotonic feature in $T_c(\mu)$ dependence due to the singularity in the density of states.

Interestingly, the Curie temperature slightly decreases with the increase in the hole density in the range of gate voltages from 40 to 50 V. This corresponds to the hole chemical potential varying from 50 to 70 meV, approximately, where, in accordance with Fig. 2(a), the heavy-hole fraction in the density of states decreases because the corresponding subband becomes more and more light-hole-like. Since the exchange interaction between carriers and magnetic ions is dominated by the heavy-hole contribution, the decrease of the heavy-hole density of states results in the decrease of the Curie temperature. We note that, for a Curie temperature of about 30 K, the corresponding exchange interaction energy is of the order of 1 meV, much smaller than the hole chemical potential ∼50 meV, which justifies the approximate expression (6) for $T_c$.

## IV. CONCLUSION

We show that the Curie temperature may be dramatically changed by a small variation of the gate voltage in specially designed doped diluted semiconductor QWs. Taking into account the peculiarities of the complex valence band in a zinc-blende semiconductor, we estimated that one can reach the Curie temperature variation by a factor of 2 with a variation of the applied voltage by about 5 V. The predicted effect is caused by the steplike variations of the density of states in the valence band in the vicinity of Lifshitz topological transitions that can be controlled by the external bias. A strong sensitivity of the Curie temperature to the applied voltage can be used in semiconductor spintronic devices, in particular in ferromagnetic switches and spin transistors.

## ACKNOWLEDGMENTS

M.M.G. is grateful to RSF Project No. 17-12-01265 for partial support. A.V. and A.K. acknowledge partial support from the HORIZON 2020 RISE project CoExAn (Grant No. 644076). Financial support from the Saint-Petersburg State University and Deutsche Forschungsgemeinschaft (DFG), Project No. 40.65.62.2017, is acknowledged.

[1] J. K. Furdyna, Diluted magnetic semiconductors, J. Appl. Phys. **64**, R29 (1988).
[2] T. Jungwirth, J. Sinova, J. Mašek, J. Kučera, and A. H. MacDonald, Theory of ferromagnetic (III,Mn)V semiconductors, Rev. Mod. Phys. **78**, 809 (2006).
[3] T. Dietl and H. Ohno, Dilute ferromagnetic semiconductors: Physics and spintronic structures, Rev. Mod. Phys. **86**, 187 (2014).
[4] T. Dietl, A. Haury, and Y. Merle d'Aubigne, Free carrier-induced ferromagnetism in structures of diluted magnetic semiconductors, Phys. Rev. B **55**, R3347(R) (1997).
[5] A. Haury, A. Wasiela, A. Arnoult, J. Cibert, S. Tatarenko, T. Dietl, and Y. Merle d'Aubigné, Observation of a Ferromagnetic Transition Induced by Two-Dimensional Hole Gas in Modulation-Doped CdMnTe Quantum Wells, Phys. Rev. Lett. **79**, 511 (1997).
[6] D. Kitchen, A. Richardella, J.-M. Tang, M. E. Flatte, and A. Yazdani, Atom-by-atom substitution of Mn in GaAs and visualization of their hole-mediated interactions, Nature (London) **442**, 436 (2006).
[7] S. Ohya, K. Takata, and M. Tanaka, Nearly non-magnetic valence band of the ferromagnetic semiconductor GaMnAs, Nat. Phys. **7**, 342 (2011).
[8] M. Dobrowolska, K. Tivakornsasithorn, X. Liu, J. K. Furdyna, M. Berciu, K. M. Yu, and W. Walukiewicz, Controlling the Curie temperature in (Ga,Mn)As through location of the Fermi level within the impurity band, Nat. Mater. **11**, 444 (2012).
[9] A. X. Gray, J. Minar, S. Ueda, P. R. Stone, Y. Yamashita, J. Fujii, J. Braun, L. Plucinski, C. M. Schneider, G. Panaccione, H. Ebert, O. D. Dubon, K. Kobayashi, and C. S. Fadley, Bulk electronic structure of the dilute magnetic semiconductor $Ga_{1-x}Mn_xAs$ through hard X-ray angle-resolved photoemission, Nat. Mater. **11**, 957 (2013).
[10] T. Ishii, T. Kawazoe, Y. Hashimoto, H. Terada, I. Muneta, M. Ohtsu, M. Tanaka, and S. Ohya, Electronic structure

near the Fermi level in the ferromagnetic semiconductor GaMnAs studied by ultrafast time-resolved light-induced reflectivity measurements, Phys. Rev. B **93**, 241303(R) (2016).

[11] T. Jungwirth, K. Y. Wang, J. Masek, K. W. Edmonds, J. König, J. Sinova, M. Polini, N. A. Goncharuk, A. H. MacDonald, M. Sawicki, A. W. Rushforth, R. P. Campion, L. X. Zhao, C. T. Foxon, and B. L. Gallagher, Prospects for high temperature ferromagnetism in (Ga,Mn)As semiconductor, Phys. Rev. B **72**, 165204 (2005).

[12] L. Chen, X. Yang, F. Yang, J. Zhao, J. Misuraca, P. Xiong, and S. von Molnár, Enhancing the curie temperature of ferromagnetic semiconductor (Ga,Mn)As to 200 K via nanostructure engineering, Nano Lett. **11**, 2584 (2011).

[13] N. V. Agrinskaya, V. A. Berezovets, A. Bouravlev, and V. I. Kozub, Ferromagnetic ordering in Mn-doped quantum wells GaAs-AlGaAs resulting from the virtual Anderson transition, Solid State Commun. **183**, 27 (2014).

[14] T. Kasuya, A theory of metallic ferro- and antiferromagnetism on Zener's model, Progr. Theor. Phys. **16**, 45 (1956).

[15] L. M. Roth, H. J. Zeiger, and T. A. Kaplan, Generalization of the Ruderman-Kittel-Kasuya-Yosida interaction for nonspherical fermi surfaces, Phys. Rev. **149**, 519 (1966).

[16] D. N. Aristov, Indirect RKKY interaction in any dimensionality, Phys. Rev. B **55**, 8064 (1997).

[17] V. I. Litvinov and V. K. Dugaev, RKKY interaction in one- and two-dimensional electron gases, Phys. Rev. B **58**, 3584 (1998).

[18] F. Matsukura, H. Ohno, A. Shen, and Y. Sugawara, Transport properties and origin of ferromagnetism in (Ga,Mn)As, Phys. Rev. B **57**, R2037(R) (1998).

[19] T. Kernreiter, M. Governale, and U. Zulicke, Carrier-Density-Controlled Anisotropic Spin Susceptibility of Two-Dimensional Hole Systems, Phys. Rev. Lett. **110**, 026803 (2013).

[20] T. Kernreiter, RKKY interaction induced by two-dimensional hole gases, Phys. Rev. B **88**, 085417 (2013).

[21] X. C. Zhang, A. Pfeuffer-Jeschke, K. Ortner, V. Hock, H. Buhmann, C. R. Becker, and G. Landwehr, Rashba splitting in n-type modulation-doped HgTe quantum wells with an inverted band structure, Phys. Rev. B **63**, 245305 (2001).

[22] H. Ohno, D. Chiba, F. Matsukura, T. Omiya, E. Abe, T. Dietl, Y. Ohno, and K. Ohtani, Electric-field control of ferromagnetism, Nature (London) **408**, 944 (2000).

[23] Ya. M. Blanter, M. I. Kaganov, A. V. Pantsulaya, and A. A. Varlamov, The theory of electronic topological transitions, Phys. Rep. **245**, 159 (1994).

[24] A. A. Varlamov, A. V. Kavokin, and Y. M. Galperin, Quantization of entropy in a quasi-two-dimensional electron gas, Phys. Rev. B **93**, 155404 (2016).

[25] J. Davies, *The Physics of Low-Dimensional Semiconductors* (Cambridge University Press, Cambridge, 1998).

[26] S. Luryi, Quantum capacitance devices, Appl. Phys. Lett. **52**, 501 (1988).

[27] I. A. Merkulov, D. R. Yakovlev, A. Keller, W. Ossau, J. Geurts, A. Waag, G. Landwehr, G. Karczewski, T. Wojtowicz, and J. Kossut, Kinetic Exchange between the Conduction Band Electrons and Magnetic Ions in Quantum-Confined Structures, Phys. Rev. Lett. **83**, 1431 (1999).

[28] P. Lawaetz, Valence band parameters in cubic semiconductors, Phys. Rev. B **4**, 3460 (1971).

[29] For the homogeneous distribution of Mn ions, the quantities $J_{hh}$, $J_{lh}$ are insensitive to the specific form of the envelope functions.

[30] L. Landau and E. Lifshitz, *Statistical Physics, Part 1* (Butterworth-Heinemann, Oxford, 2000).

[31] I. A. Merkulov, V. I. Perel', and M. E. Portnoi, Momentum alignment and spin orientation of photoexcited electrons in quantum wells, Zh. Eksp. Teor. Fiz. **99**, 1202 (1991) [JETP **72**, 669 (1991)].

[32] L. E. Vorob'ev, D. V. Donetskii, and L. E. Golub, Absorption and emission of far-IR radiation by hot holes in GaAs/AlGaAs quantum wells, Pis'ma Zh. Eksp. Teor. Fiz. **63**, 928 (1996) [JETP Lett. **63**, 977 (1996)].

[33] I. L. Aleiner and E. L. Ivchenko, Anistropic exchange splitting in type II GaAs/AlAs superlattices, JETP Lett. **55**, 692 (1992); E. L. Ivchenko, A. Yu. Kaminski, and U. Rössler, Heavy-light hole mixing at zinc-blende (001) interfaces under normal incidence, Phys. Rev. B **54**, 5852 (1996); M. V. Durnev, M. M. Glazov, and E. L. Ivchenko, Spin-orbit splitting of valence subbands in semiconductor nanostructures, *ibid.* **89**, 075430 (2014).

[34] G. Friesen, E. D. Dunlop, and R. Wendt, Investigation of CdTe solar cells via capacitance and impedance measurements, Thin Solid Films **387**, 239 (2001).

[35] We note that, with further increase in the manganese content, other effects related to Mn-clustering, formation of the impurity band, and increase of the disorder in the sample, become pronounced.